

# Intercalation of salicylic acid into ZnAl layered double hydroxides by ionic-exchange method

M. SILION (FRUNZA), D. HRITCU, M. I. POPA\*

Department of Chemical Engineering, Faculty of Chemical Engineering, Technical University Iasi, Bd. D. Mangeron 71A, 700050, Iasi, Romania

Salicylic acid was intercalated into ZnAl-layered double hydroxides lamella as an inorganic host by ion exchange technique. The intercalation compound was examined by X-ray diffraction (XRD), FTIR spectroscopy, differential thermal analysis and thermo gravimetric analysis. Powder X-ray diffractogram shows that the basal spacing of the ZnAl layered double hydroxide with salicylate as the intergallery anion expanded from 8.7 Å to 15.4 Å. The  $\text{NO}_3^-$  peak located at  $1385\text{ cm}^{-1}$  in FTIR spectra was displaced in the sample with peaks characteristic to the intercalated salicylate. The thermal stability of the intercalated salicylic acid is significantly enhanced compared with the pure form before intercalation.

(Received June 01, 2009; accepted July 20, 2009)

**Keywords:** Layered double hydroxide, Ion exchange, Intercalation, Salicylic acid

## 1. Introduction

The class of materials known as layered double hydroxides (LDHs) or hydrotalcite-like materials have the general formula:  $[M_{1-x}^{2+}M_x^{3+}(OH)_2]^{x+}A_{x/m}^{m-} \cdot zH_2O$ , where  $M^{2+} = \text{Mg, Zn, Ca, Co, Fe, Ni, Cu, etc.}$ ,  $M^{3+} = \text{Al, Fe, Cr, Ga, etc.}$ ,  $A^{m-} = \text{Cl}^-, \text{CO}_3^{2-}, \text{NO}_3^-, \text{etc.}$ ,  $m$  is the formal charge of anion and  $x$  is the stoichiometric coefficient that can be widely varied. As it can be seen from the formula, the formal positive charge of the layer depends on the  $M^{2+}/M^{3+}$  ratio. These materials have many applications as catalysts, optical and electrical functional materials [1, 2].

Due to the ability to exchange the interlayer anion, the layered double hydroxides may be used as biocompatible hosts for several drugs, such as NSAID (non-steroidal anti-inflammatory drugs), widely used in rheumatism treatment, which very often show adverse secondary effects, such as gastric and duodenal ulcers formation.

In the literature was reported several pharmaceutically active compounds such as diclofenac, gemfibrozil, ibuprofen, ketoprofen, naproxen, etc. could be reversibly intercalated into LDH for their storage and controlled release [3-8].

LDHs - based controlled release systems have also been studied [9-14]. In this work we have investigated the intercalation behavior of salicylic acid (Sal) into ZnAl-LDHs by ion-exchange reaction. Salicylic acid is used in rheumatism treatment, but its adverse secondary effects, such a gastric and duodenal ulcer formation are quite common. The effect of LDHs in preventing taurcholate induced gastric injury in rat was demonstrated in the literature [15]. Salicylic acid was intercalated into MgAl-LDHs by reconstruction and coprecipitation method [16].

## 2. Experimental

### 2.1 Materials

All chemicals including  $\text{Zn}(\text{NO}_3)_2 \cdot 6\text{H}_2\text{O}$ ,  $\text{Al}(\text{NO}_3)_3 \cdot 9\text{H}_2\text{O}$ , NaOH were analytical grade. Salicylic acid was purchased from Aldrich.

### 2.2 Preparation ZnAlLDH

100 ml of an aqueous solution of  $\text{Zn}(\text{NO}_3)_2 \cdot 6\text{H}_2\text{O}$  (0.2mol)/ $\text{Al}(\text{NO}_3)_3 \cdot 9\text{H}_2\text{O}$  (0.1mol) and an aqueous solution of NaOH 1M, were mixed together by drop wise addition. During the whole process the flow was controlled in such a way that the pH was kept at a constant value of 8.5. The resulting white precipitate was aged at 338 K for 24 h under stirring. After the ageing step, the precipitate was separated by centrifugation, washed extensively with warm deionized water until sodium free and dried under vacuum at  $40^\circ\text{C}$ .

### 2.3 Preparation of Sal-LDH hybrid materials

Salicylate – layered double hydroxides nanocomposite samples were prepared by anion exchange reaction. 150 ml of 0.1M Sal aqueous solution were added into 250 ml aqueous dispersion containing 1g ZnAl-LDH under nitrogen atmosphere and vigorous magnetic stirring. The pH of the mixture was held constant at 8.0 by simultaneous addition of 1M NaOH solution. The exchange reaction was allowed to proceed at room temperature for 24 h.

The obtained precipitates were filtered, washed with deionized water and dried at  $37^\circ\text{C}$ .

## 2.4 Characterization

Powder X-ray diffraction (XRD) was performed on a Bruker AXS D8 diffractometer using CuK  $\alpha$  radiation ( $\lambda = 0.154$  nm) at 40 KV and 35 mA between  $4^\circ$  and  $70^\circ$  ( $2\theta$ ) with a graphite secondary monochromator. Fourier-transform infrared (FTIR) spectra were recorded on a Bomem MB 104 spectrophotometer on pressed KBr pellets. Thermogravimetric analysis (TG, DTG and DTA) were recorded a Netzsch TG 209C thermogravimetric analyzer at a typical rate  $10^\circ$  C/min under air atmosphere. The molecular modeling studies were performed using the Hyperchem software package.

## 3. Results and discussion

### 3.1 Powder X-ray diffraction (XRD)

The powder XRD patterns of the precursor ZnAl-LDH and the sample produced by reaction of Sal with LDH are shown in Fig. 1. The ZnAl-LDH precursor has an XRD pattern similar to those reported previously [17], with a basal spacing ( $d_{003}$ ) of 8.7 Å (Fig. 1a). After reaction with Sal, the powder XRD pattern of the product maintains the major characteristic features of ZnAl-LDH (Fig. 1b). The main diffraction peaks of Sal-ZnAl-LDH structure appear at  $5.07^\circ$ ,  $11.7^\circ$  and  $17.5^\circ$ , with an expanded basal spacing ( $d_{003}$ ) of 15.4 Å. The diffraction peak at 15.4 Å is assigned the  $d_{003}$ , proving that the guest molecules are lying horizontally to the hydroxide region in a monolayer.

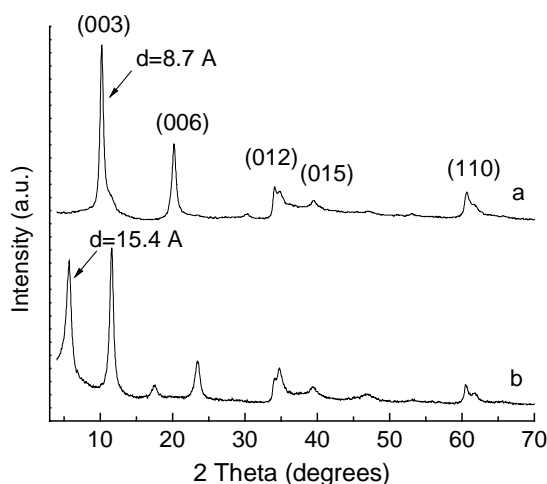


Fig. 1. The XRD spectra (a) ZnAl LDH, (b) Sal-ZnAl-LDH.

The peak at  $17.5^\circ$   $2\theta$  might be the reflection of the unchanged LDH precursor, this indicates that there is very little of the unexchanged LDH-nitrate phase remaining in the product. The peak at  $11.7^\circ$   $2\theta$  is the superposition of (003) reflection of the precursor and (006) reflection of the intercalation product, accounting for its enhanced intensity.

The reflections can be indexed to a hexagonal lattice with R-3m rhombohedral symmetry, commonly used for the description of the LDH structures. Table 1 lists the gallery height and lattice parameters.

Table 1. Lattice parameters and gallery height.

Sample	$d_{003}$ (Å)	c (Å)	a (Å)	Gallery height (Å)
ZnAl-LDH	8.7	26.2	3.06	3.9
Sal-ZnAl-LDH	15.4	46,2	3.058	10.6

### 3.2 FTIR spectroscopy

The insertion of Sal in the lamella of ZnAl-LDH is also confirmed by FTIR spectroscopy (Fig. 2). All the vibration bands of the organic anion are observed together with the absorption bands of ZnAl-LDH. The FTIR spectrum of the ZnAl-LDH is shown in Fig. 2 (a). The absorption band at around  $3431$   $\text{cm}^{-1}$  is attributed to the OH stretching due to the presence of hydroxyl group of LDH and/or physically adsorbed water molecule. The appearance of a strong band at  $1381$   $\text{cm}^{-1}$  can be assigned to the  $\nu_3$  nitrate group, the counter anion in the ZnAl-LDH. The band at  $1626$   $\text{cm}^{-1}$  is due to  $\nu(\text{H-O-H})$  band vibration. As shown in Fig. 2 (a), ZnAl-LDH is free of carbonate anion.

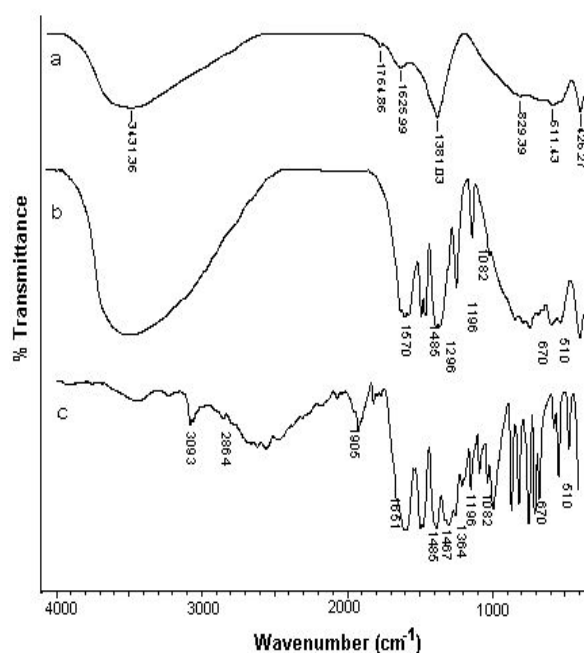


Fig. 2. FTIR spectra (a) ZnAl LDH, (b) Sal, (c) Sal-ZnAl-LDH.

Two other bands at 611 and  $426$   $\text{cm}^{-1}$  can be attributed to the Al-OH and ZnAl-OH bending vibration [18, 19], respectively. Salicylic acid shows a spectrum with many absorption bands (Fig.2b).

In addition to bands at high wave number values, due to  $\nu(\text{OH})$  and  $\nu(\text{=C-H})$  moieties, a band is recorded at  $1651$   $\text{cm}^{-1}$ , due to mode  $\nu(\text{C=O})$  of the acid group; the

abnormally low intensity of this band is due to intramolecular hydrogen bonds. The bands due to  $\nu(\text{C}-\text{C})$  of the aromatic ring are recorded at 1583, 1485, and 1467  $\text{cm}^{-1}$ ; those due to modes  $\nu(\text{C}-\text{O})$  and  $\delta(\text{O}-\text{H})$  of the acid and alcohol functions are recorded at 1296, 1240, and 1290  $\text{cm}^{-1}$ , while in-plane and out-of-plane  $\delta(\text{CH})$  bands are recorded below 1000  $\text{cm}^{-1}$  [20].

The spectrum recorded after incorporation of the Sal is presented in Fig.2c. Due to the ionization of the acid group, the band previously detected for free Sal at 1651  $\text{cm}^{-1}$  disappears, while a new band is recorded at 1570  $\text{cm}^{-1}$ . The appearance of this band is caused by the  $\nu_{\text{as}}(\text{COO}^-)$  mode. Another band recorded at 1364  $\text{cm}^{-1}$  is due to the symmetric vibration.  $\nu_{\text{s}}(\text{COO}^-)$ . The band originated from the  $\delta(\text{CH}_3)$  mode is recorded at 1386  $\text{cm}^{-1}$ . The band assigned to the nitrate group (1381  $\text{cm}^{-1}$ ) had lower intensity after the ion-exchange reaction, supporting the assumption that  $\text{NO}_3^-$  anion was replaced by Sal. The other bands are recorded in positions very close to those previously shown for free Sal. In addition, bands due to Zn/Al- OH translational modes are recorded.

### 3.3 Thermal stability

The TG and DTG curves of the LDHs and Sal-ZnAl-LDH are depicted in Fig. 3 and Fig. 4. The total loss was 39% in the case of the LDHs as a reference sample and 48% for Sal-ZnAl-LDH.

The steps up to 200°C are due to the removal of the interlayer water molecules. They are quite strongly attached to the hydroxide layer and/or interlayer anion via hydrogen bonds and the interlayer balancing anion  $\text{NO}_3^-$ .

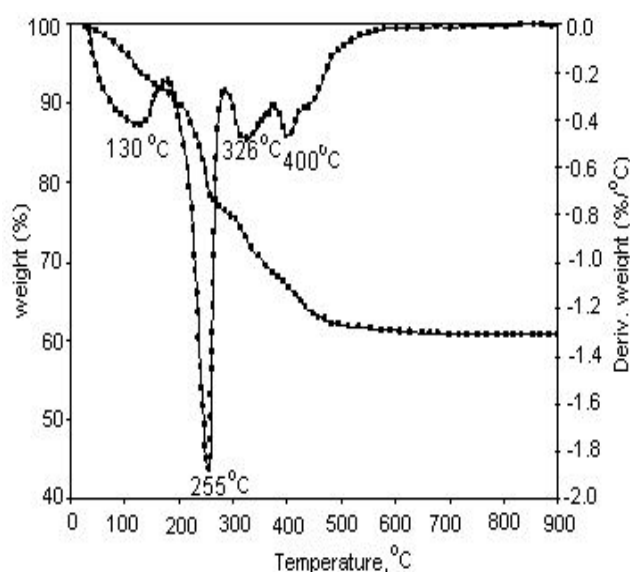


Fig. 3. The TG-DTG analysis ZnAl-LDH.

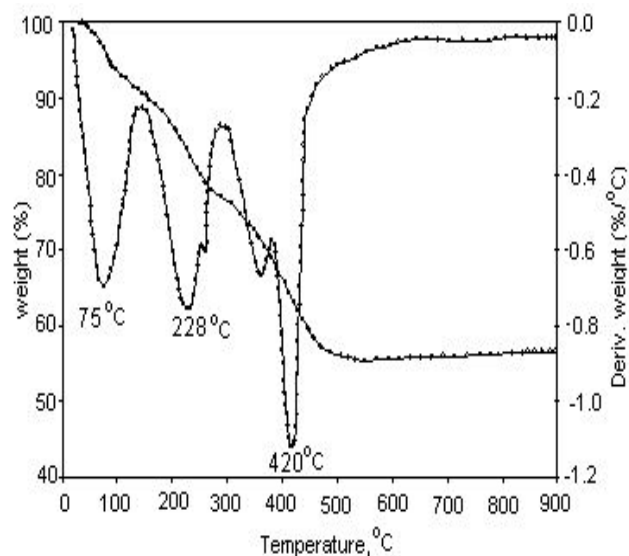


Fig. 4. The TG-DTG analysis Sal-ZnAl-LDH.

The presence of microspores is confirmed on DTG plots. Indeed the desorption of the adsorbed water molecules from the intercalates appear as two separate events for Sal-ZnAl-LDH and as a continuous step for ZnAl-LDH. The observed mass loss in the higher temperature range from 220 to 450°C is attributed to the dehydroxylation of the ZnAl-LDH basal layer. The TG curve of Sal-LDHs (Fig.4) clearly shows a rapid weight loss between 330° and 430°C.

This event is attributed to the decomposition of the Sal intercalated and to the dehydroxylation of ZnAl-LDH. From TG curve it is easily observed that the mass loss in the region 350-430°C of Sal-LDHs is 20.3%. Furthermore, it is noted that Sal anions were completely decomposed above 420° C. This proves the enhanced thermal stability of intercalated Sal due to the host-guest interaction between lamella of ZnAl-LDH.

### 3.4 Structural modeling

The molecular dimension of Sal compound, calculated using the chemical bond lengths and atomic angles (using Hyperchem software), is 5.12 Å along the y-axis and 6.6 Å along the x-axis. According to the XRD data, the intercalation of the Sal molecule leads to an increase of the interlayer distance to 10.6 Å for the Sal-ZnAl-LDH sample.

The proposed orientation of the Sal anions is presented in Fig. 5. The model takes into account the length of the hydrogen bonds established between the anions and the LDH hydroxyl groups.

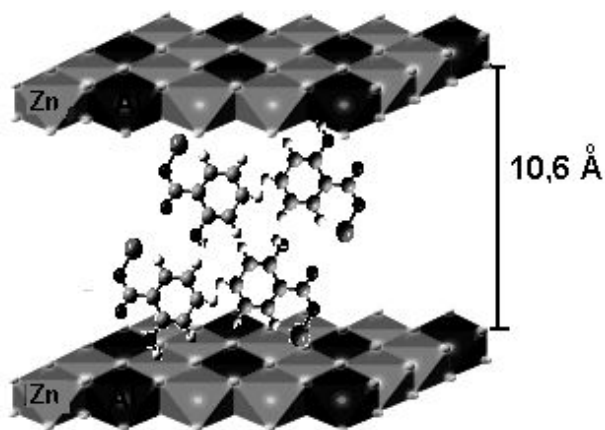


Fig. 5. Schematic illustration of layered nanohybrid.

#### 4. Conclusions

Sal-LDH was obtained by the intercalation of Sal anions into zinc-aluminium layered double hydroxide by ion exchange reaction. XRD diffractometry and FTIR spectroscopy methods were used to confirm the intercalation structure. The basal spacing recorded was 8.7 Å for simple LDHs. Upon incorporation of salicylic acid into zinc hydroxide layer, the intercalative monohybrid had basal spacing of 15.4 Å. In the FTIR spectra, the band characteristic for nitrate group showed lower intensity due to the replacement with Sal anions. The thermal stability of Sal was improved by intercalation.

#### References

- [1] V. Rives, Nova Science Publishers, New York, 365, 2001.
- [2] A. Vaccari, *Appl. Clay Sci.* **14**, 161 (1999).
- [3] V. Ambrogi, G. Fardella, G. Grandolini, L. Perioli, *Int. J. Phar.* **220**, 23 (2001).

- [4] M. Del Arco, E. Cebadera, S. Gutierrez, C. Martin, M. J. Montero, V. Rives, J. Rocha, M. A. Sevilla, *J. Pharm. Sci.* **93** (6), 1649 (2004).
- [5] M. Del Arco, S. Gutiérrez, C. Martín, V. Rives, J. Rocha, *J. Solid State Chem.* **177**, 3954 (2004).
- [6] Z. Wang, E. Wang, L. Gao, L. Xu, *J. Solid State Chem.* **178**, 736 (2005).
- [7] H. Zhang, K. Zou, H. Sun, X. Duan, *J. Solid State Chem.* **178**(11), 3485 (2005).
- [8] S. H. Hwang, Y. S. Han, J. H. Choy, *Bull. Korean. Chem. Soc.* **22**(9), 1019 (2001).
- [9] M. Frunza, G. Lisa, R. Zonda, M. I. Popa, *Rev. Chim.* **59**(4), 409 (2008).
- [10] M. Del Arco, A. Fernandez, C. Martin, V. Rives, *Appl. Clay Sci.* **42**, 538 (2009).
- [11] F. P. Bonina, M. L. Giannossi, L. Medici, C. Puglia, V. Summa, F. Tateo, *Appl. Clay Sci.* **41**, 165 (2008).
- [12] U. Constantino, V. Ambrogi, M. Nocchetti, L. Perioli, *Micropor. Mesopor. Mat.*, **107**, 149 (2008).
- [13] B. Li, J. He, D. G. Evans, X. Duan, *Appl. Clay Sci.* **27**(3-4), 199 (2004).
- [14] A. I. Khan, L. Lei, A. J. Norquist, D. O'Hare, *Chem. Commun.*, 2342 (2001).
- [15] M. Frunza, G. Carja, M. I. Popa, *Scientific Study and Research* **VI**(2), 173 (2005).
- [16] B. P. Yu, J. Sun, M. Q. Li, H. S. Luo, J. P. Yu, *World J. Gastroenterol.* **9**, 1427 (2003).
- [17] M. Z. Hussein, Z. Zainal, A. H. Yahaga, *J. Contr. Rel.* **82**, 417 (2002).
- [18] Z. P. Xu, H. C. Zeng, *J. Phys. Chem. B* **105**, 1743 (2001).
- [19] S. Velu, V. Amukumar, V. Narayanan, C. S. Swamy, *J. Mat. Sci.* **32**, 957 (1997).
- [20] S. Kanan, C. S. Swamy, *J. Mat. Chem. Lett.* **11**, 1585 (1992).
- [21] L. J. Bellamy, *The Infrared Spectra of Complex Molecules*, Chapman and Hall, London, 1975.

\*Corresponding author: mipopa@ch.tuiasi.ro